IOP Conf. Series: Materials Science and Engineering **382** (2018) 032042 doi:10.1088/1757-899X/382/3/032042

Normal Stiffness model of bolted joint based on the modified three-dimensional elastic-plastic contact fractal model

Yunyao Yin, Ligang Cai, Zhifeng Liu*, Yongsheng Zhao, Qiang Cheng

Institute of Advanced Manufacturing and Intelligent Technology, Beijing University of Technology, Beijing 100124, China

Mechanical Industry Key Laboratory of Heavy Machine Tool Digital Design and Testing, Beijing University of Technology, Beijing 100124, China

E-mails: liuzfbjut@163.com

Abstract. Bolted joints have a significant effect on the dynamical behaviour of assembled structures. Accurate contact stiffness model of bolted joint is crucial in predicting the dynamic performance of bolted structures. In this research, a modified three-dimensional fractal model of normal contact stiffness is presented to more accurately predict the dynamic characteristic of a bolted assembly. In the present model, while the contact deformation exceed the critical value the elastic-plastic contact is used to take the place of Hertz elastic contact in the traditional M-B model, and revise the drawback that elastic-plastic contact occurs before elastic contact in existing elastic-plastic fractal models. As the increase of contact force, the plastic deformation of single asperity is considered again, which is omitted in the two type fractal models. An experimental set-up with two T-shaped specimen is designed conducted to verify the efficiency of the proposed model. Comparing with the ZX elastic-plastic fractal model, the present model can predict contact stiffness and dynamic performance more accurately, particularly, while for higher contact loads. The results show that the modified elastic-plastic fractal contact model can be used to more accurately predict the stiffness and dynamic characteristic of bolted structures in the machine tools.

1. Introduction

The dynamic behaviour of bolted structure plays a significant role in determining the machining stability and precision of a machine tool. The study shows that up to 90% of the system damping is provided by the joints, and 60% of the system stiffness comes from the joints[1]. The bolted joint is one of the weakest parts of the machine tool. The dynamic behavior of bolted joint is can be affected by the geometry and machining precision of contract surface, property of material and external load. The micro-contact theory can describe the relationship of the preload, surface roughness, and material characteristics, it make it possible to accurately model bolted joints and to optimize bolted assemblies.

The micro-contact mechanics of bolted joints is based on the geometry topography of surface and Hertz

contact theory. Fractal geometry has been widely used to study engineering surfaces exhibiting random, multi-scale topographies and self-affinity[2]. Majumdar and Bushan[3] developed one of the first fractal contact models describe the contact of rough surfaces (referred to in the following as the MB model). Komvopoulos and Yan[4] developed a three-dimensional fractal contact model, based on MB model(referred to in the following as the KY model), to calculate the contact load and contact area of rough surface. Some elastic-plastic contact models[5, 6] were proposed, based on the Hertz contact

model. Lin [6] determine the elastoplastic regime of a spherical asperity in terms of the interference of two contact surfaces (LL model). Kogut and Etsion [5] gave the more detailed division for the elastic-plastic deformation area into two stages, using finite element method. Wen and Zhang[7, 8] built up the fractal model for normal contact stiffness of machine joint surfaces, based on the M-B model, which Hertz contact theory between a sphere and a plane and the contact fractal theory between rough surfaces. Li[9] introduced a three-dimensional fractal model of normal contact stiffness of joint surface, the the friction factor was also coincided in normal contact stiffness fractal prediction model. Zhao and Xu[10, 11] proposed a 3D elastic-plastic model (ZX model), based on YK model and LL model, and obtain the normal stiffness with uneven pressure distribution[12]. While contact pressure over a critical value, only elastic deformation is be coincided, in all models based on the traditional M-B model. In addition, existing elastic-plastic fractal models also suffers from a drawback that, the transition of the contact and deformation state are from elastic-plastic to elastic.

In this paper, a modified three-dimensional contact stiffness fractal model is proposed. Instead of Hertz elastic contact, as the increase of contact pressure, elastic-plastic contact and plastic deformation are also coinsided in present model. An experimental set-up with two bolted specimens is designed for validating the presented model. The normal stiffness are assigned to the MATRIX 27 element for analyzing the dynamic characteristic of bolted assembly, using ANSYS soft. The experimental natural frequency and mode shape are compared with the presented model and YX model. The results show that, the present model can predict contact stiffness and dynamic performance more accurately, particularly, while the preload is greater. The presented model can be used to more accurately predict the stiffness and dynamic characteristic of bolted structures in the machine tools.

2. The modified elastic-plastic fractal contact model

The machined surface is continuity, non-differentiability and statistically self-affinity. These mathematical properties are satisfied by the two-dimensional Weierstrass-Mandelbrot (W-M) function given in M-B fractal contact model[2, 3]. Yan[4] and Komvopoulos[13] extended M-B fractal contact model to a three-dimensional contact model given by:

$$z(x) = L\left(\frac{G}{L}\right)^{(D-2)} \left(\ln\gamma\right)^{0.5} \sum_{n=n_0}^{n_{\max}} \gamma^{(D-3)n} \left[\cos\varphi_n - \cos\left(\frac{2\pi\gamma^n x}{L} - \varphi_n\right)\right] \tag{1}$$

where the parameters x, y are the planar Cartesian coordinates, D is the fractal dimension of surface profile, ($1<D<2$). G represents fractal roughness parameter. γ is dimension parameter of the spectral density (γ=1.5). L is the sampling length, φ_n is the random phase. n is frequency index, $n_{\max}$ is the upper limit of n. With the base wavelength and the corresponding frequency index n_0.

$$n_0 = \text{int}\left[\frac{\log\left(L/2r'\right)}{\log\gamma}\right],$$

And then, the W-M function for the single asperity can be written as,

$$z_0(x) = G^{(D-2)} \left(\ln\gamma\right)^{\frac{1}{2}} \left(2r'\right)^{(3-D)} \left[\cos\varphi_{1,n_0} - \cos\left(\frac{\pi x}{r'} - \cos\varphi_{1,n_0}\right)\right] \tag{2}$$

2.1 The modified elastic-plastic contact model of asperity

The asperity interference δ for single asperity is equal to the peak-to-valley amplitude of the cosine function $z_0(x)$. For a given contact spot with an truncated area ($a'=\pi r'^2$), the δ can be given as[14, 15]

$$\delta = 2^{4-D} \pi^{\frac{D-3}{2}} \left(\ln\gamma\right)^{\frac{1}{2}} G^{D-2} a'^{\frac{3-D}{2}} \tag{3}$$

With the relationship $\left(r'\right)^2 = 2R\delta$, the equivalent radius of curvature R can be written as

$$R = \frac{a'^{(D-1)/2}}{2^{(5-D)} \pi^{(D-1)/2} G^{(D-2)} (\ln\gamma)^{1/2}} \tag{4}$$

According to Chang and Etsion[16], the critical deformation thickness δ_c corresponding to the yielding behaviour is expressed as

$$\delta_c = \left(\frac{\pi kH}{2E}\right)^2 R \tag{5}$$

where k is the hardness coefficient, and H is hardness of the soft material. k is the coefficient related with the passion ratio v, and can be written as k=0.454+0.41v.

As defined, the critical contact area can be obtained as:

$$a_c' = \left[\frac{2^{11-2D} G^{2(D-2)} (\ln\gamma) E^2}{\pi^{(4-D)} (kH)^2}\right]^{\frac{1}{D-2}} \tag{6}$$

Kogut and Etsion[5] extend contact model of asperity to elastoplastic regime in a range of $1<\delta/\delta_c<110$. With a distinct transition in the contact behavior at δ/δ_c=6, the elastoplastic regime was divided into the first ($1<\delta/\delta_c<6$) and second elastoplastic ($6<\delta/\delta_c<110$) regimes.

According to Eq.(3), the dimensionless interference values δ/δ_c is obtained

$$\frac{\delta}{\delta_c} = \left(\frac{a'}{a_c'}\right)^{\frac{3-D}{2}} \tag{7}$$

Be differ from the existing elastic-plastic fractal model in Refs[10, 15] , δ/δ_c is expressed as:

$$\frac{\delta}{\delta_c} = \left(\frac{a_c'}{a'}\right)^{(D-2)} \tag{8}$$

Eq.(8) is be inconsistent with Eq. (3), it is means that Eq.(8) is unreasonable to used in fractal model.

The critical contact area, a_{ep}' at δ/δ_c=6 and a_p' at δ/δ_c=110, can be expressed as, respectively.

$$a_{ep}' = 6^{\frac{2}{3-D}} a_c' \tag{9}$$

$$a_p' = 110^{\frac{2}{3-D}} a_c' \tag{10}$$

According to M-B fractal model and other fractal models based on M-B contact theory[7, 12, 17], with $a' > a_c'$, asperity is in elastic deformation regime, and Hertz theory is adopted to describe the contact characteristic. In this paper, according to Eq.(7), while $a' > a_c'$, $\delta > \delta_c$ is obtained. Instead of Hertz elastic contact, K-E elastic-plastic contact model is adopted in the range of $a_c' \le a' \le a_{ep}'$.

Substituting Eqs. (6-8) into the relationship of contact load f, area a and the dimensionless interference δ/δ_c , in KE model, the relationship of contact load f, area a and contact truncated area a' can be obtained, as follows:

(1) In the first elastoplastic deformation regime ($a_c' \le a' \le a_{ep}'$)

$$f_{ep1} = H_1 a'^{(1.85-0.425D)} \tag{11}$$

(2) In the second elastoplastic deformation regime ($a_{ep}' \le a' \le a_p'$)

$$f_{ep2} = H_2 a'^{(1.526-0.263D)} \tag{12}$$

Where H_1, and H_2 are the parameter related with the fractal parameters and material properties, respectively, can be expressed as.

$$H_1 = 0.68 \cdot 2^{(3.675-0.85D)} \pi^{(0.425D-1.7)} (\ln\gamma)^{0.425} (KH)^{0.15} E^{0.85} G^{(0.85D-1.7)}$$

$$H_2 = 0.93 \cdot 2^{(1.893-0.526D)} \pi^{(0.263D-1.052)} (\ln\gamma)^{0.263} (KH)^{0.474} E^{0.526} G^{(0.526D-1.052)}$$

In the deformation regime $\delta > \delta_c$ ($a' \ge a_p'$), asperity is in the fully plastic deformation regime. Besides, introduced by models based on M-B fractal model[3, 4, 7, 12], the deformation of asperity is also

assumed as fully plastic deformation, while $a' < a'_c$. The contact truncated area and contact load of a single asperity in the fully plastic deformation regime are written respectively as

$$f_p = Ha' \tag{13}$$

Summing up the above, the normal contact load of asperity, in deformation regime, can be rewritten as follows:

$$f = \begin{cases} f_p & a'_p \le a' \\ f_{ep2} & a'_{ep} \le a' < a'_p \\ f_{ep1} & a'_c \le a' < a'_{ep} \\ f_p & 0 < a' < a'_c \end{cases} \tag{14}$$

2.2 Contact analysis of rough surface

The three-dimensional size distribution function of whole micro-contacts, can be written as[11, 15, 17]

$$n(a') = \frac{D-1}{2}\psi^{(3-D)/2} a_l'^{(D-1)/2}\, a'^{(-D-1)/2} \tag{15}$$

where, a'_l denotes the maximum of truncated area of a surface. Ψ is domain extension factor, can be obtained with the transcendental equation as follows:

$$\frac{\psi^{(3-D)/2} - (1+\psi^{(1-D)/2})^{-(3-D)/(D-1)}}{(3-D)/(D-1)} = 1.$$

The total normal load in the first elastic-plastic regime can be obtained as

$$F_{ep1} = \int_{a'}^{a'_{ep}} f_{ep1} n(a') da' = \frac{(D-1)H_1\psi_c^{(3-D)/2}}{2(2.35-0.925D)} a_l'^{(D-1)/2}\left[a_{ep}'^{(2.35-0.925D)} - a_c'^{(2.35-0.925D)}\right] \tag{16}$$

The total normal load in the second elastic-plastic regime can be obtained as

$$F_{ep2} = \int_{a'_{ep}}^{a'_p} f_{ep2} n(a') da' = \frac{(D-1)H_1\psi_c^{(3-D)/2}}{2(2.026-0.763D)} a_l'^{(D-1)/2}\left[a_p'^{(2.026-0.763D)} - a_{ep}'^{(2.026-0.763D)}\right] \tag{17}$$

The total normal load in first fully plastic regime can be expressed as

$$F_{p1} = \int_0^{a'_c} f_p n(a') da' = \frac{D-1}{3-D}\psi^{(3-D)/2} Ha'_c \qquad (0 < a' < a'_c) \tag{18}$$

The total normal load in second fully plastic regime can be expressed as

$$F_{p2} = \int_{a'_{ep}}^{a'_l} f_p n(a') da' = \frac{D-1}{3-D}\psi^{(3-D)/2} Ha_l'^{(D-1)/2}\left[a_l'^{(3-D)/2} - a_p'^{(3-D)/2}\right] \qquad (a' > a'_p) \tag{19}$$

Summing up the above, the normal contact load of asperity, can be rewritten as follows:

$$F = \begin{cases} F_{ep1} + F_{ep2} + F_{p1} + F_{p2} & a'_l > a'_p \\ F_{ep} + F_{ep2} + F_{p1} & a'_{ep} < a'_l < a'_p \\ F_{p1} + F_{ep1} & a'_c < a'_l < a'_{ep} \\ F_{p1} & 0 < a'_l < a'_c \end{cases} \tag{20}$$

3. Normal contact stiffness of bolted joint

3.1 Normal contact stiffness of asperity

According to the definition of the contact stiffness, the contact stiffness of a single asperity can be expressed as

$$k_n = \frac{df/da'}{d\delta/da'} \tag{21}$$

Substituting Eqs.(3, 11-12) into Eq.(21), contact stiffness, in first and second elastoplastic deformation regimes, can be written as

$$k_{nep1} = \frac{H_1 \pi^{(3-D)/2}(1.85-0.425D)}{2^{3-D}(3-D)G^{D-2}(\ln\gamma)^{1/2}} a'^{(0.35+0.075D)} \tag{22}$$

$$k_{nep2} = \frac{H_2 \pi^{(3-D)/2}(1.526-0.263D)}{2^{3-D}(3-D)G^{D-2}(\ln\gamma)^{1/2}} a'^{(0.026+0.237D)} \tag{23}$$

3.2 contact stiffness of bolted joint

The total normal stiffness K_n can be given by integrating in the whole contact surface as

$$K_n = K_{nep1} + K_{nep2} \tag{24}$$

Where K_{nep1} *and* K_{nep2} are the normal stiffness in first and second elastoplastic deformation regimes.

$$K_{nep1} = \int_{a_c'}^{a_{ep}'} k_{nep1} n(a') da' \tag{25}$$

$$K_{nep2} = \int_{a_{ep}'}^{a_p'} k_{nep2} n(a') da' \tag{26}$$

Substituting Eqs. (15, 22-23) into Eq. (25-26), the total normal stiffness K_n can be rewritten as

$$K_n = H_1 H_{G1} a_l'^{(D-1)/2}(a_{ep}'^{(0.85-0.425D)} - a_c'^{(0.85-0.425D)}) + H_2 H_{G2} a_l'^{(D-1)/2}\left[a_p'^{(0.526-0.263D)} - a_{ep}'^{(0.526-0.263D)}\right] \tag{27}$$

Where the parameters H_{G1}, and H_{G2}, can be expressed as.

$$H_{G1} = \frac{(1.85-0.425D)(D-1)\pi^{(3-D)/2}\psi^{(3-D)/2}}{(0.85-0.425D)2^{4-D}(3-D)(\ln\gamma)^{1/2}G^{D-2}} \text{ and } H_{G2} = \frac{(1.526-0.263D)(D-1)\pi^{(3-D)/2}\psi^{(3-D)/2}}{(0.526-0.263D)2^{4-D}(3-D)(\ln\gamma)^{1/2}G^{D-2}}$$

4. The experimental set-up and validation of the bolted joint model

In order to verify the effectiveness of the presented contact model, the bolted specimens are designed as shown in Fig.1. First, the natural frequency of the bolted specimen was experimentally determined. Secondly, the contact pressure of bolted joint can be obtained in the FE method, then, the largest truncated area a_l' can be calculated by using Eq. (20). Substituting a_l' into Eq.(27), the normal stiffness of the contact surface can be obtained. Finally, numerical values of normal stiffness was then assigned to MATRIX27 element of the FE model, which is used to connect the node-to-node of two contact surfaces. The FEM results were compared with the experimental results.

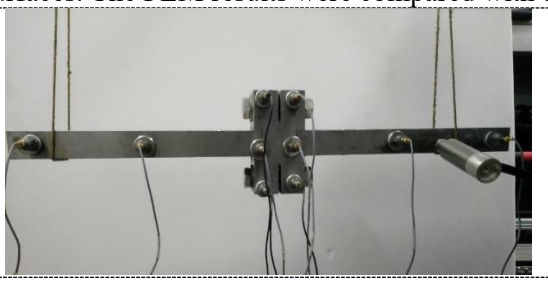

Figure 1. Experimental set-up of bolted joint.

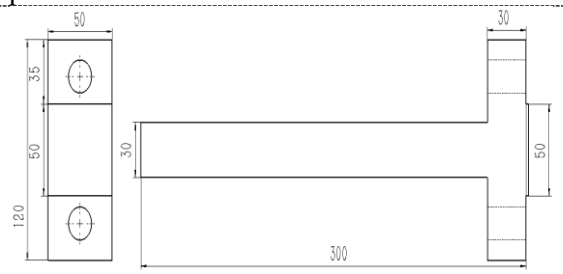

Figure 2. Test specimen and Dimensions.

4.1 Experimental Set-up and Experimental Principle

The assembled experimental structure consisted of two T type specimen connected with two steel structure bolts (M16). The dimensions and material properties of the T type specimen are shown in Fig. 2 and Table 1, respectively. The LMS Test.lab vibration testing and analysis system was adopted to acquire and analyse the signals of model knocking test, and the first nature frequency was obtained.

The elastic modulus (E), Passion ratio (v), and density of specimen are 210 GPa, 0.28 and 7800 kg/m^3, respectively.

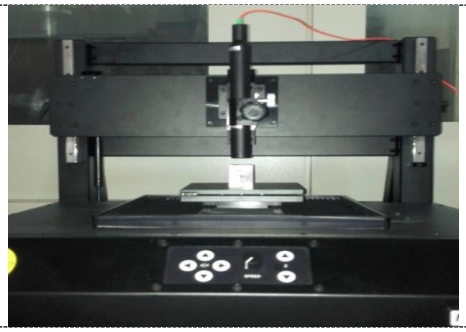

Figure 3. Scanning specimen surface.

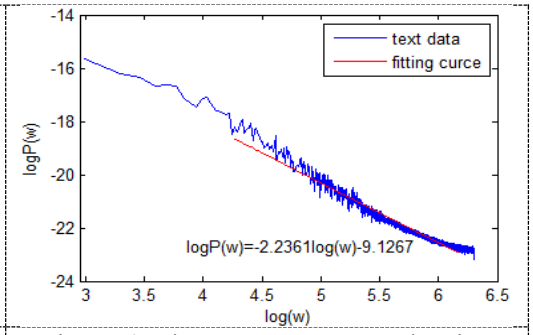

Figure 4. The power spectrum density.

The surface was scanned by using the NANOVEA three dimensional surface Profiler, as show in Fig. 6. The power spectrum density of the test surface is shown in Fig. 7. By means of the power spectrum density method, we obtained the 2D fractal dimension D_s and fractal roughness parameter. D_s=1.383 and G=8.589×10^{-13}. The three-dimensional fractal dimension D= D_s+1.

4.2 Verification of the presented model

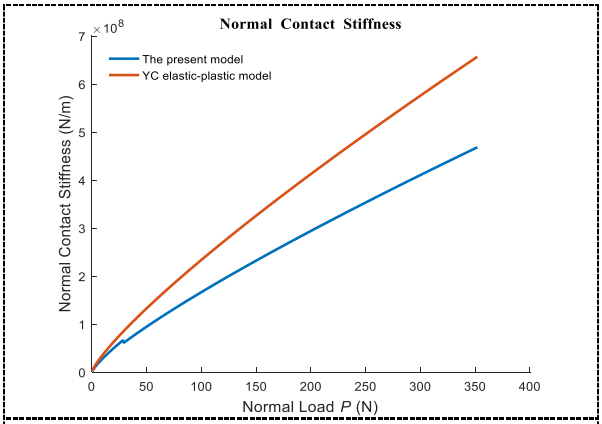

Figure 5. The comparison of normal stiffness

Fig. 5 shows that, the normal contact stiffness of bolted joint can be improved by the increase of preload.

The contact stiffness obtained by the present model and YC model, under different normal load, are showing in Fig. 5. It is interesting to note that, under lower loads the present model results are in good agreement with the YC results. It should be noted that, while for higher contact loads, the present results gradually step away from the YC results, and obtain lower stiffness values. A gap of stiffness appear for F values (about 30), in the present model. This may be because that, according to KE model, the contact loads have a small difference to each other in the first and second elastic-plastic regime at the critical value δ/δ_c=6.

Table 1. Natural frequencies of the bolted assembly adopting different model

Pre-tightening force of bolt	5 KN	25 KN	40 KN
Experimental results	522.86	588.26	602.23
Results adopting the proposed model	519.79	592.68	604.63
Error value with experimental results	3.67	4.42	2.4
Results adopting Y-C model	521.62	594.21	613.21
Error value with experimental results	1.24	5.95	10.98

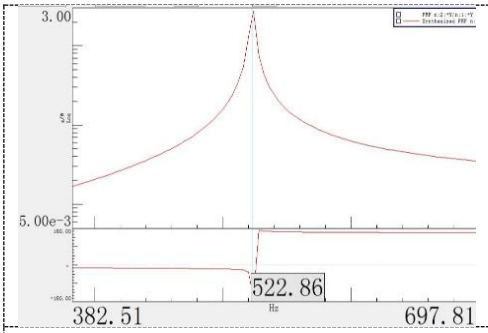

(a) Pre-tightening force 5 KN

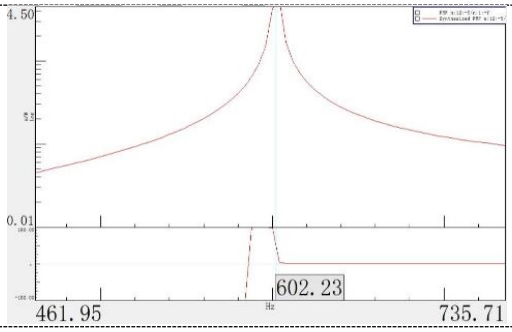

(a) Pre-tightening force 40 KN

Figure 6. The natural frequency value obtained by model experiment.

The first-order natural frequency value obtained by model experiment are showing in Fig. 6 . Fig. 7 shows the simulated modal shape and nature frequency with the presented model, Fig 8 correspond to the Y-C model. The 1st order natural frequencies of bolted assembly adopting different bolted joint model, under different force, are shown in Table 1. Comparing with the experimental results under the same force, it can thus be seen that, for the presented model, the error values of the 1st order natural frequencies of bolted assembly are 3.67, 4.42, and 2.4, respectively, under the force are 5 KN, 25 KN, 40 KN. As to the YC elastic-plastic model, the error values are 1.24, 5.95 and 10.98. It is interesting to note that under lower contact loads the YC model is more accurate than the present model. While for higher loads the YC become less accurate, as increases of the loads, the error values also gradually become larger. The comparison results indicate that the presented model can better meet the requirements for predicting the dynamic characteristic of an assembly with bolted joints, accurately.

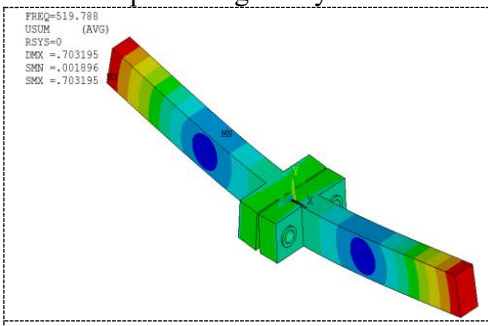

(a) Pre-tightening force 5 KN

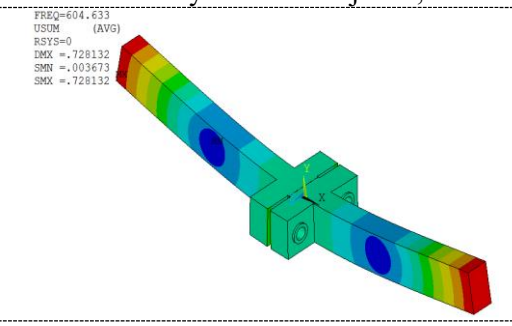

(a) Pre-tightening force 40 KN

Figure 7. Simulated modal shape and nature frequency with the presented model

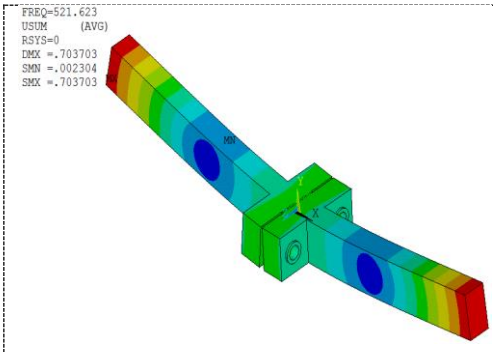

(a) Pre-tightening force 5 KN

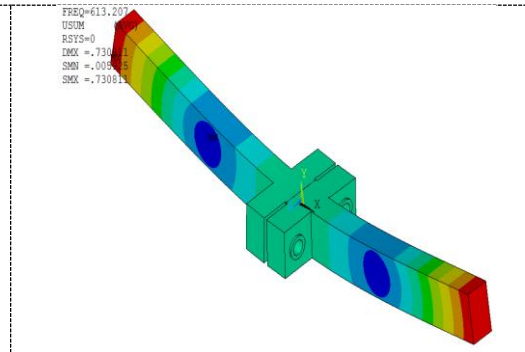

(a) Pre-tightening force 40 KN

Figure 8. Simulated modal shape and nature frequency with the Y-C model

5. Conclusion

A modified three-dimensional fractal model of elastic-plastic contact is established in this paper. The normal stiffness of contact surface for the bolted joint is obtained. Revising the drawback of MB fractal models and the existing elastic-plastic fractal models, that only elastic deformations were considered under higher contact loads. While contact loads beyond the critical values, elastic-plastic deformation and plastic deformation were also considered in present model. Comparing the first-order natural frequencies of the bolted structure obtained by the present model and the Y-C elastic-plastic fractal model, severally, with the experimental results. The comparisons show that the present model is more accuracy for predicting the contact stiffness and dynamic performance of bolted structures, particularly, while under higher contact loads. The proposed method greatly improve the prediction accuracy of stiffness for bolted joints, which can be better applied to predict the dynamic properties of bolted structure in the design stage.

Acknowledgments

This work was supported by National Natural Science Foundation of China (No. 51575008).

Reference

[1] Ibrahim R.A., Pettit C.L.2005 Uncertainties and dynamic problems of bolted joints and other fasteners. *Journal of Sound and Vibration*, 279(35): 857-936
[2] A M and CL T 1990 Fractal characterization and simulation of rough surfaces *Wear* 136 313-27
[3] Majumdar A and Bhushan B 1991 Fractal Model of Elastic-Plastic Contact Between Rough Surfaces *Journal of Tribology* 1-11
[4] Yan W and Komvopoulos K 1998 Contact analysis of elastic-plastic fractal surfaces *Journal of Applied Physics* 7 3617-24
[5] Kogut L and Etsion I 2002 Elastic-Plastic Contact Analysis of a Sphere and a Rigid Flat *Journal of Applied Mechanics and Technical Physics* 657-62
[6] Lin LP, Lin JF, Lin LP and Lin JF 2006 A New Method for Elastic-Plastic Contact Analysis of a Deformable Sphere and a Rigid Flat *Journal of Tribology*
[7] Zhang X, Wang N, Lan G, Wen S and Chen Y 2014 Tangential Damping and its Dissipation Factor Models of Joint Interfaces Based on Fractal Theory With Simulations *Journal of Tribology* 011704 1-10
[8] Zhang X, Wang N, Lan G and Wen S 2014 Elastoplastic fractal model for normal contact stiffness of rough surfaces with continuous critical contact parameters *JOURNAL OF VINRATION AND SHOCK* 09 72-7
[9] Pan W, Li X, Wang L, Guo N and Mu J 2017 A normal contact stiffness fractal prediction model of dry-friction rough surface and experimental verification *European Journal of Mechanics - A/Solids* 94-102
[10] Zhao Y, Xu J, Cai L, Shi W and Liu Z 2016 Stiffness and damping model of bolted joint based on the modified three-dimensional fractal topography *Proceedings of the Institution of Mechanical Engineers, Part C: Journal of Mechanical Engineering Science*
[11] Zhao Y, Xu J, Cai L, Shi W, Liu Z and Cheng Q 2016 Contact characteristic analysis of spindle-toolholder joint at high speeds based on the fractal model *Proceedings of the Institution of Mechanical Engineers, Part E: Journal of Process Mechanical Engineering*
[12] Zhao Y, Yang C, Cai L, Shi W and Hong Y 2016 Stiffness and Damping Model of Bolted Joints with Uneven Surface Contact Pressure Distribution *Strojniški vestnik - Journal of Mechanical Engineering* 11 665-77
[13] Komvopoulos K and Ye N 2001 Three-Dimensional Contact Analysis of Elastic-Plastic Layered Media With Fractal Surface Topographies *Journal of Tribology* 632-40
[14] Liou JL and Lin JF 2010 A modified fractal microcontact model developed for asperity heights with variable morphology parameters *Wear* 1-2 133-44
[15] Ji C, Zhu H and Jiang W 2013 Fractal prediction model of thermal contact conductance of rough

surfaces *Chinese Journal of Mechanical Engineering* 1 128-36
[16] Chang WR and Etsion I 1987 An Elastic-Plastic Model for the Contact of Rough Surfaces
[17] Xiaopeng Li BYGZ 2014 Fractal Prediction Model for Normal Contact Damping of Joint Surfaces considering Friction Factors and Its Simulation *Advances in Mechanical Engineering*